ISRG Journal of Engineering and Technology (ISRGJET)

ISRG PUBLISHERS

Abbreviated Key Title: ISRG J Eng Technol

ISSN: 3107-5894 (Online)

Journal homepage: https://isrgpublishers.com/isrgjet/

Volume – II Issue- IV (July – August) 2026

Frequency: Bimonthly

Novel Design of Solar Carport with Tracking System: A Case Study of Baghdad, Iraq

Mustafa F. Yousif[1*], Ali K. Hassan[2], Ali S. Khasaal[3], Doaa R. Hussain[4], Hussien D. Salman[5]

[1, 2, 3, 4, 5] Training and Energy Research Office, Ministry of electricity, Baghdad, Iraq

| **Received:** 05-08-2026 | **Accepted:** 10-08-2026 | **Published:** 12-08-2026

*__Corresponding author: Mustafa F. Yousif__

Abstract

In particular, solar energy is a strong substitute since it reduces reliance on non-renewable resources and offers economic and environmental benefits. However, because it needs to accommodate a lot of parking spaces and provide the most energy feasible, constructing a solar-powered carport could be difficult. Simultaneously, the design of parking spots must adhere to several regulations, and the design of photovoltaic systems must take several things into account. With a novel motion mechanism, the current study intends to build a sun-tracking solar carport that tilts at more angles, increasing the amount of incident irradiance and electrical power generated by the panels. Two distinct sun-tracking solar carport designs with distinct motion mechanisms were designed, the first with a single column mechanism and the second with an X -shape mechanism, After identifying the suitable location for the solar carport for the Training and Energy Research Department at the Ministry of Electricity in Baghdad, Iraq, In January 2024, from 8 AM to 4 PM, the stress, deformation, and variation in solar irradiance impinge on the panels between the horizontal and tilted carport were examined and assessed. The findings demonstrated that, in terms of solar irradiance, the sun-tracking solar carport has a larger percentage than the fixed carport. The X-shaped solar carport design has a maximum equivalent stress of 145 MPa, whereas the single-column mechanism solar carport has a maximum equivalent stress of 112.45 MPa. The X-shaped solar carport design has a maximum deformation of 4.797 mm, whereas the single-column mechanism solar carport design has a maximum deformation of 29.65 mm. Consequently, in terms of sun-tracking angles and their capacity to tolerate stress and deformation, the second design—the X-shaped mechanism that has been suggested is the most appropriate for working.

Keywords: *Design, Solar carport, Tracking, Energy, Solar angle*

DOI: 10.5281/zenodo.21897816

1. Introduction

The necessity of finding renewable energy solutions has never been more urgent. Concerns about climate change, coupled with the finite nature of traditional fossil fuel resources, underscore the urgent need to transition to sustainable energy sources [1]. Solar energy, in particular, represents a compelling alternative, offering not only environmental benefits but also economic advantages by reducing reliance on non-renewable resources [2]. However, designing a solar carport can be difficult, because it needs to do its job to accommodate a good amount of parking space and generate as much energy as possible. At the same time, many rules must be followed while designing parking spaces, and many factors must be considered while

designing photovoltaic systems [3]. On the other hand, the effectiveness of solar carports largely depends on their ability to efficiently capture and convert solar radiation into usable energy. Sun-tracking technology addresses this challenge by dynamically adjusting the orientation of solar panels to align with the sun's position throughout the day. By continuously optimizing the angle of incidence, sun tracking systems can significantly enhance the energy yield of solar installations, thereby maximizing their efficiency [4]. In ideal conditions, single-axis trackers can achieve efficiency gains of 20% to 30% [5][6]. However, these numbers can vary depending on factors such as the latitude of the site, climate, and specific characteristics of the solar panels and tracking technology used. The design and installation of solar carports can significantly impact the efficiency of solar panel systems. A study by Hwang et al. [7] found that the energy yield of a bifacial module system in a solar carport was 3.08% higher than that of a mono-facial system due to rear-side absorption. Another study by Deka et al. [8] concluded that vertically oriented carport systems were the most efficient solar rooftop systems for humid subtropical areas. Additionally, Vandewetering et al. [9] conducted a study on PV parking lot canopies and found that these systems can provide a low-cost solution for EV charging, with single-span systems providing cost savings of 82-85%. An investigation by Chen and Xie [10] the stress, strain and maximum deformation of original model are analyzed in industrial conditions, to achieve a significant reduction of the maximum deformation and to satisfy the engineering requirements. These findings highlight the importance of considering the design and orientation of solar carports in order to maximize the energy efficiency of solar panel systems. This paper aims to delve into the intricacies of solar carport sun tracking systems, exploring their design principles, operational mechanisms, and the impact of various factors on their performance. Through a comprehensive review of existing literature, case studies, and possibly simulations or experimental data, we seek to elucidate the efficacy of sun tracking technology in the context of solar carports.

2. Methodology

The right location for the solar carport's design and the fundamental dimensions of the parking spots was first determined. The quantity of energy produced by the panels and the incident solar irradiance were compared between the tilted and horizontal carports. The solar carport's mechanical construction design. The solar carport's solar panel type and specifications.

2.1. The Carport Location and Parking Regulations

The projected solar carport that was the focus of this study is situated in the Ministry of Electricity's Training and Energy Research Department in Baghdad, Iraq. There are four parking spaces available to the Training and Energy Research Department; Figure 1 illustrates which one is most suited for the installation of the solar carport. Since it does not move in accordance with the sun azimuth angle, the fourth parking spot is not appropriate. Because of the surrounding structures and trees, parking spots 1 and 2 might offer a lot of shade. As a result, parking spot 3 could be the best choice for installing the solar carport. The application of the solar carport in the current study is based on the typical parking spot size [11], as indicated in Figure 2, and takes into consideration the high-profile vehicles (SUVs) [12], as indicated in Figure 3.

Figure 1. the installation of the solar carport

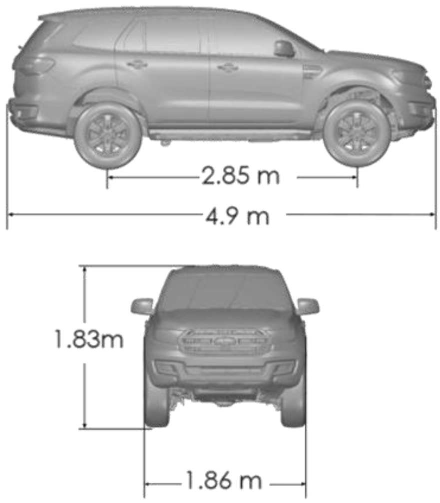

Figure 2. the typical parking spot size

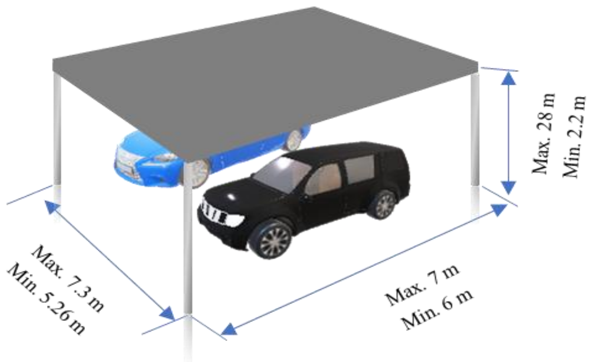

Figure 3. the high-profile vehicles (SUVs)

DOI: 10.5281/zenodo.21897816

2.2. The Horizontal and Tilted Carport

Generally speaking, slanted solar panel usage is preferable to fixed or horizontal solar panel positioning. Because they spend more time in the light during the noon hours, solar panels that are slanted exhibit superior performance in terms of electrical energy generation. [13,14] As a result, the two types of solar carports that were the subject of the current study were fixed and sun-tracking (solar tilt angle). To find out which style of carport is more effective at boosting the solar panel's ability to produce electricity, a comparison of the two was conducted. As indicated in Table 1 and Figure 4, the investigation was carried out for the sun angles and solar radiation for January 2024 from 8 AM to 4 PM. As a consequence of the sun-tracking solar carports' greater solar radiation ratio as compared to the fixed carports, the power they produce is superior to that of the stationary carports, according to the data. Because sun-tracking carports are more productive, it is the subject of the current study. Using the formulas found in the appendix, the solar irradiance and tilt angles were computed.

Table 1. comparison between horizontal and tilted carport

Time	Horizontal [W/m^2]	Tilted	
8	472.29	807.87	71.05%
9	652.59	884.57	35.55%
10	794.06	910.44	14.66%
11	883.91	913.46	3.34%
12	914.69	916.47	0.20%
13	883.91	913.46	3.34%
14	794.06	910.44	14.66%
15	652.59	884.57	35.55%
16	472.29	807.87	71.05%

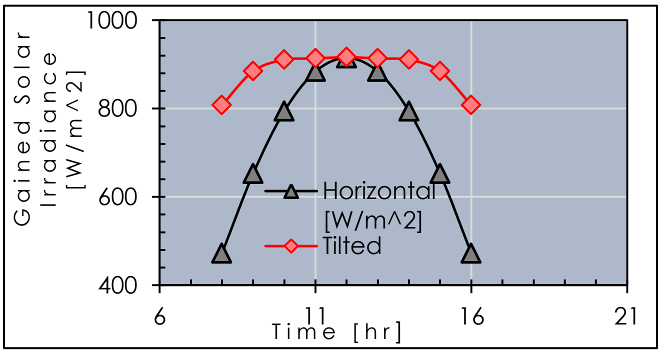

Figure 4. comparison between horizontal and tilted carport

2.3. Design and Mechanical Structure of Models

To get the ideal tilt angle for the solar carport, two distinct kinds of sun-tracking solar carports with various mechanical movement mechanisms were created using the SolidWorks version 2020 program.

2.3.1. Design Model I (single column mechanism)

As seen in Figure 5, a sun-tracking solar carport was developed with dimensions of 4.5 meters by 7 meters, which allowed for the parking of two cars, and a height of 4 meters to get the ideal tilt angle. To optimize the capture of solar irradiance, the tilt angle was determined to be 35 degrees, as seen in Figure 6. The solar carport moves in both the southeast and southwest directions. A 3.5-meter-tall circular shaft with a diameter of 6 inches was employed, and it was set within a reinforced concrete base measuring 60 by 60 by 60 cm.

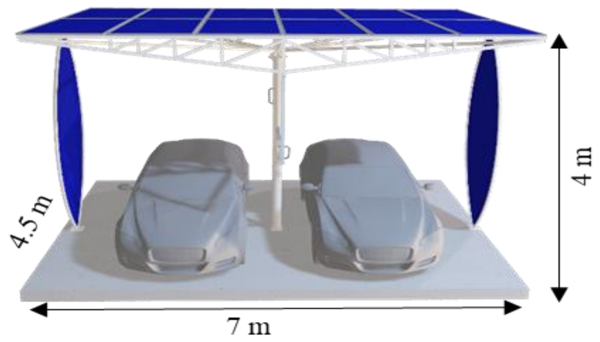

Figure 5. Design Model I (single column mechanism)

A two-inch-diameter circular shaft goes through the carport's three supports, one at the top of the shaft and the other two on its sides. The carport is supported by a 4-inch square steel frame, and the solar panels are mounted in a 6x2 matrix on an aluminum frame, for a total of 12 solar panels. To enable two-way movement, movement arms are fastened to the circular shaft's sides; the tilt angle is measured using a protractor. Details of the solar carport design are shown in Figure 7.

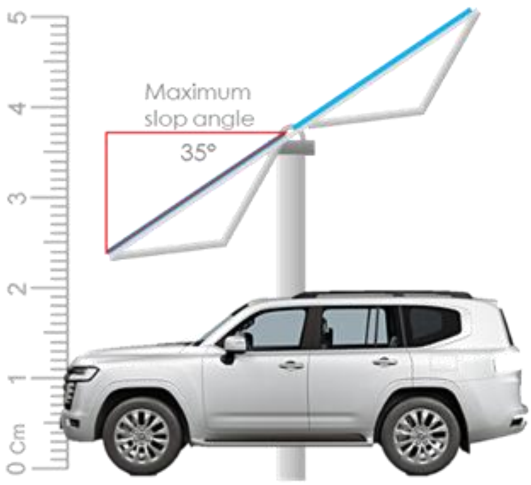

Figure 6. maximus of tilt angle of design Model I

2.3.2. Design Model II (X -shape mechanism)

The dimensions of the second design match those of the first design that was discussed in the preceding section. As seen in Figure 8, the distinction lies in the sun-tracking solar carport's construction and movement mechanism. This design's movement mechanism is based on a movement system with links, and the links are made of square-section steel (2 x 2 x 0.25 inches). These links also act as a mechanical support system to keep the sun-tracking solar carport's construction from collapsing. The offset distance between the brackets permits whole intersection movement without causing a collision, and it was taken into consideration to prevent collisions caused by the carport's movement. The sides were fastened to a (500 x 30 x 60 cm) reinforced concrete slab. There are a total of 12 solar panels installed in a 2-column, 6-row matrix, mounted on an aluminum

DOI: 10.5281/zenodo.21897816

frame. The concrete foundation, measuring 60 x 60 x 60 cm, was used to secure the movement link of the solar carport. This foundation allows the carport to move in two directions. The link was fastened with a handle. The solar carport's movement mechanism is designed to tilt it at angles ranging from 0 to 60 degrees. All of the design elements for the solar carport are displayed in Figure 9.

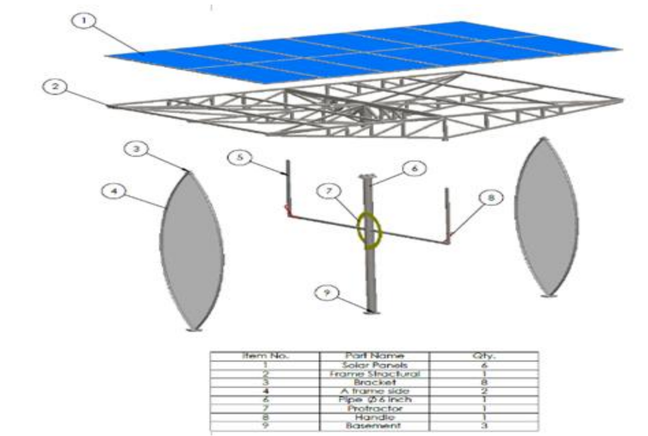

Figure 7. Details of the solar carport design

(a)

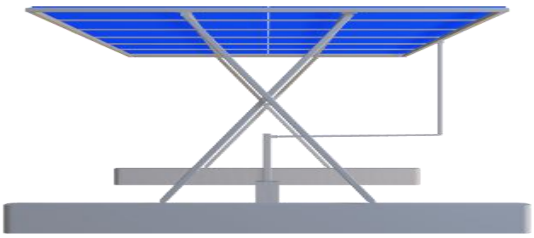

(b)

Figure 8. Design Model II (X -shape mechanism), (a) front shape, (b) side shape

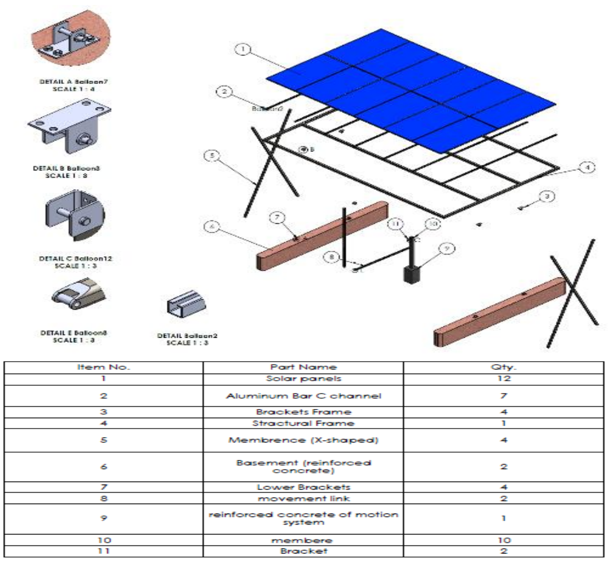

Figure 9. Details of the solar carport design

2.4. Solar Panel PV Specification

Longi solar panels with a 550-watt capacity were employed in this investigation. As seen in Figure 10, there are twelve solar panels mounted on the sun-tracking solar carports, with the following measurements for each panel: 2278 x 1134 x 35 mm. Tables 2 and 3 provide all the information and characteristics of the solar panel that was employed.

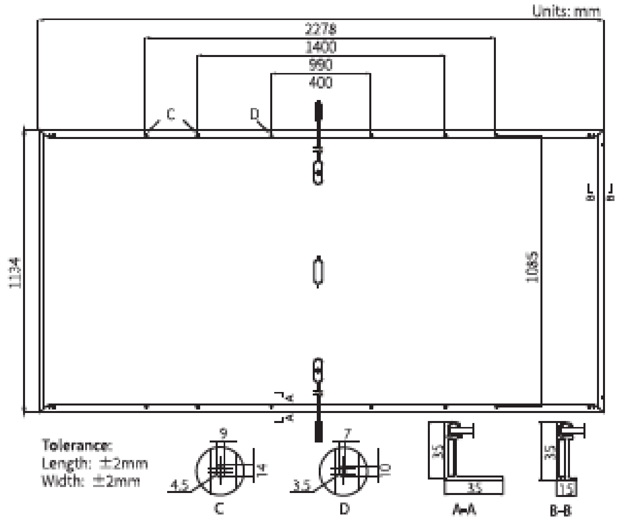

Figure 10. Demention of solar panel

Table 2. electrical characteristics

Module type	**LR5-72HPH-550M**	
Testing condition	**STC**	**NOCT**
Maximum power (Pmax/W)	550	411.1
Open circuit voltage (Voc/V)	49.80	46.82
Short circuit current (Isc/A)	13.98	11.31
Voltage at maximum power (Vmp/V)	41.95	38.97
Current at maximum power (Imp/A)	13.12	10.56
Module efficiency (%)	21.3	

Table 3. operating parameters

Operation	**Parameters**
Operational temperature	-40 °C - + 85 °C
Power output tolerance	0-3 %
Voc and Isc tolerance	±3%
Maximum system voltage	DC1500V (IEC/UL)
Maximum series fuse rating	25A
Normal operating cell temperature	45±2 °C
Protection class	Class II
Fire rating	UL Type 1 or 2 IEC Class C

DOI: 10.5281/zenodo.21897816

3. Result and discussion

ANSYS version 20 software was utilized to do numerical simulations of the sun-tracking solar carports to discuss and evaluate the findings. This was done to assess the mechanical characteristics of the carport and its capacity to bear the loads and strains brought on by the solar panels, the structure, and the tilting mechanism. Thus, by placing weights on the solar carport, the impact of stresses and deformations on the carport was investigated. To get excellent convergence and precision in the numerical results [16], a hexahedral mesh with 1,318,047 elements was created for the numerical analysis. The mesh generation for the sun-tracking solar carport is seen in Figure 11.

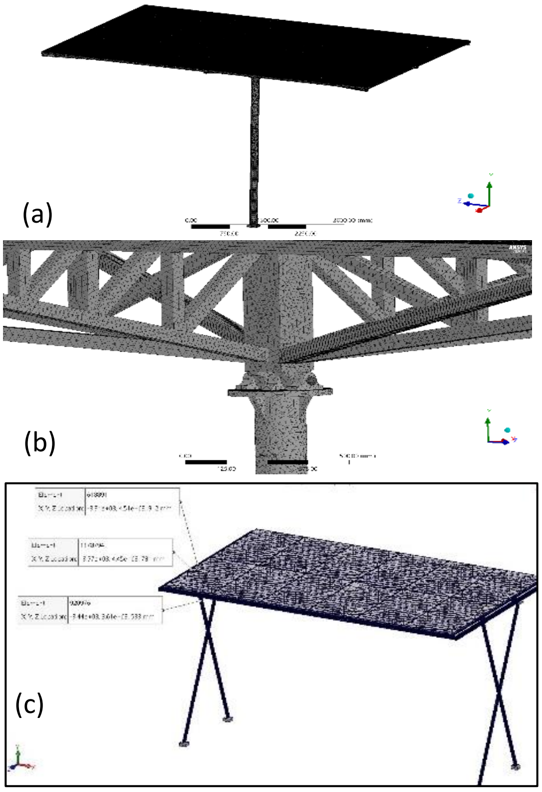

Figure 11. The mesh generation for the sun-tracking solar carport, (a) and (b) design I, (c) design II

3.1. Effect of Equivalent Stress on Solar Carport (Two Designs)

ANSYS's static analysis in mechanical engineering, equilibrium is attained without taking time-dependent factors into account. The structure response is studied under static stresses. It is frequently employed in the assessment of the structural stability, strength, and safety of different engineering systems. The Von Mises yield criteria states that a material won't begin to break as long as its highest value of strain energy density doesn't go over the amount needed to generate the material in a tensile test. A material will not yield if the highest value of the von Mises stress does not surpass the yield strength of the material [17,18]. The von Mises stress is an equivalent stress value that is used to assess if a certain material will start to yield. The formula below illustrates how the von Mises stress is often applied to ductile materials like metals [19]. The equivalent stress of the solar carport (first design) is depicted in Figure 12. The findings reveal that the largest equivalent stress, which has a maximum value of 112.45 MPa, occurs in the areas of the circular shaft connection with the solar carport's steel frame. This figure is less than the 220 MPa yield stress of the metal that was utilized to create the carport. As seen in Figure 13, the comparable stress for the second solar carport design, on the other hand, is around 145 MPa, which is also less than the yield stress of the metal utilized.

$$\sigma_v = \sqrt{\frac{(\sigma_1-\sigma_2)^2+(\sigma_2-\sigma_3)^2+(\sigma_3-\sigma_1)^2}{2}} \qquad (1)$$

Where; σ_v= equivalent stress (Von Mises stress)

σ_1 , σ_2 and σ_3= principal stress

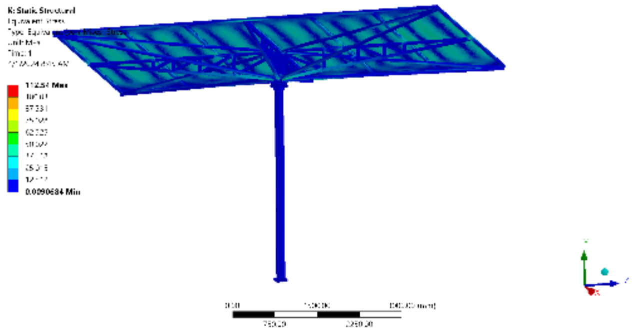

Figure 12. The equivalent stress of the solar carport (first design)

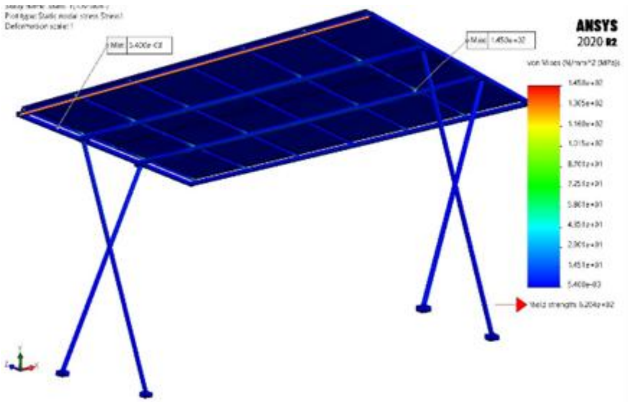

Figure 13. The equivalent stress of the solar carport (second design)

3.2. Effect of Deformation on Solar Carport (Two Designs)

Structural deformation and the idea of strain are connected in engineering. The term "strain" refers to the form change that a geometric structure's constituent parts may experience when an external load is applied. The amount of elongation or deformation that a structure may experience under various loading scenarios may be estimated using stress [20,21]. The topic of discussion in the current study was how to calculate deformation using the numerical solution, which is represented mathematically by the following equation [22]. The deformation of the solar carport for the first design is shown in Figure 14, where the findings indicate that the borders of the upper supporting structure for the solar panels experience the largest distortion, with a value of 29.65 mm. Considering that the carport follows the course of the sun, this figure is seen as favorable. As seen in Figure 15, the deformation in the second design, on the other hand, is 4.797 mm, which is a satisfactory value for the carport's capacity to bear the applied loads.

$$\delta = \frac{\Delta L}{L_o} \qquad (2)$$

DOI: 10.5281/zenodo.21897816

Where; $\Delta L = L_o - L_f$

L_o= original length

L_f = final length

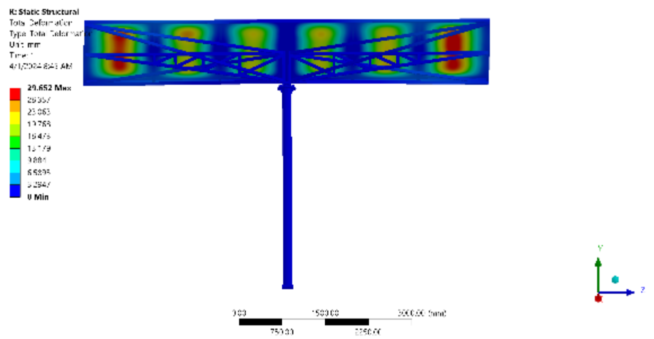

Figure 14. The deformation of the solar carport (first design)

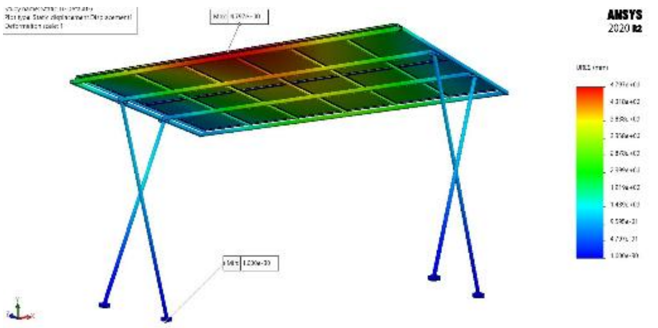

Figure 15. The deformation of the solar carport (second design)

4. Conclusions

The study looked at how much solar irradiance and electrical energy produced by the panels differed between the tilted and horizontal solar carports from 8 AM to 4 PM in January 2024. This was done after deciding on the best location for the solar carport at the Ministry of Electricity's affiliated Training and Energy Research in Baghdad, Iraq, and taking into account the sun path above the circle. This served as the basis for the design of two distinct sun-tracking solar canopy types with various motion motors. After analyzing the stress and deformation of both designed carports, the following findings were made:

1. In terms of solar irradiance ratio, the sun-tracking solar carports outperform the stationary carports in terms of power generation. This is because the former has a greater ratio than the latter.
2. The tilt angle values for the two designs (the X-shaped design and the single-column design) vary from 0 to 60 degrees, and from 0 to 35 degrees, respectively.
3. The solar carport's single-column design has a maximum equivalent stress of 112.45 MPa, whereas the X-shaped design has a maximum equivalent stress of approximately 145 MPa. The yield stress of the iron employed in the carport design, which is 220 MPa, is greater than these values for the suggested designs.
4. The maximum deformation of the solar carport's first design, a single column, is approximately 29.65 mm, but the maximum deformation of the second design, which is X-shaped, is 4.797 mm. These values for the proposed canopies are regarded as satisfactory regarding the canopy's capacity to support the applied loads.

Authors' contribution

All authors contributed equally to the preparation of this article.

Declaration of competing interest

The authors declare no conflicts of interest.

Funding source

This study didn't receive any specific funds.

Data availability

The data that support the findings of this study are available from the corresponding author upon reasonable request.

Acknowledgements

The authors would like to acknowledge …….

References

1. IPCC, 2022: Climate Change 2022: Impacts, Adaptation, and Vulnerability. Contribution of Working Group II to the Sixth Assessment Report of the Intergovernmental Panel on Climate Change [H.-O. Pörtner, D.C. Roberts, M. Tignor, E.S. Poloczanska, K. Mintenbeck, A. Alegría, M. Craig, S. Langsdorf, S. Löschke, V. Möller, A. Okem, B. Rama (eds.)]. Cambridge University Press, Cambridge, UK and New York, NY, USA. https://doi.org/10.1017/9781009325844.
2. Majeed, Muhammad and Anwar, Awais and Luni, Tania, "The Impact of Renewable and Non-Renewable Energy Consumption on Economic Growth: A Global Perspective with Developed and Developing Economies", Pakistan Journal of Commerce and Social Science, 2021, vol. 15, pp. 286-307. http://hdl.handle.net/10419/237079
3. Etukudoh, Emmanuel and Nwokediegwu, Zamathula and Umoh, Aniekan and Ibekwe, Kenneth and Ilojianya, Valentine and Adefemi, Adedayo, "Solar power integration in Urban areas: A review of design innovations and efficiency enhancements", World Journal of Advanced Research and Reviews,2024, vol. 21, pp. 1383-1394. https://doi.org/10.30574/wjarr.2024.21.1.0168
4. Lewandoski, Cristiano and Ferreira Santos, Reginaldo and Ikpehai, Augustine, "THE ADVANTAGES OF SOLAR TRACKER", International Journal of Environmental Resilience Research and Science, 2021, Vol.3. https://doi.org/10.48075/ijerrs.v3i1.26451
5. Lewandoski, C.F., Santos, R.F., Sio, J.P.M.K., Canfild, D. da C., Carmo, M.B. do., Silva, F.M. da., Siqueira, J.A.C., Oliveira, W.A. de., Ikpehai, A. and Reginatto, R, "Study of the Efficiency of the Solar Tracker System compared to the Fixed Solar Generation System", Research, Society and Development, 2022, Vol.11, no. 6. https://doi.org/10.33448/rsd-v11i6.28671
6. Gutiérrez, Sebastián and Rodrigo, Pedro and Alvarez, Jerónimo and Acero Trevethan, Arturo and Montoya, Alejandro, "Development and Testing of a Single-Axis

DOI: 10.5281/zenodo.21897816

Photovoltaic Sun Tracker through the Internet of Things", Energies, 2020, Vol.13. https://doi.org/10.3390/en13102547

7. Sungho Hwang, Yoonmook Kang, Hae-seok Lee,“ Performance and energy loss mechanism of bifacial photovoltaic modules at a solar carport system”, Energy Science & Engineering, 2020, vol. 11, pp. 2866- 2884. https://doi.org/10.1002/ese3.1497

8. N. Deka, M. R. Hazarika and S. Bharadwaj, “ Performance analysis of solar rooftop systems based on racking arrangements in humid subtropical areas IEEE International Power and Renewable Energy Conference, 2022, pp. 1-5. https://doi.org/10.1109/IPRECON55716.2022.10059488

9. Vandewetering, N.; Hayibo, K.S.; Pearce, J.M, " Open-Source Photovoltaic—Electrical Vehicle Carport Designs " Technologies, 2022, vol.10. https://doi.org/10.3390/technologies10060114

10. ChenZuobing and XIE Qiang, " Study and Design on Optimization of Carport Structure based on ANSYS ", Applied Mechanics and Materials, 2013, vol.318, pp. 182-184. http://dx.doi.org/10.4028/www.scientific.net/AMM.318.182

11. Young, W, " Parking principles: Some thoughts on the design of parking lots", Aust. Road Res, 1987, vol.17, pp. 132–136. https://trid.trb.org/View/1194745

12. Highway Research Board, " Parking Principles; Special Report 125", Natl Academy Pr., USA, 1971. https://onlinepubs.trb.org/Onlinepubs/sr/sr125.pdf

13. J. Polo, S. Garcia-Bouhaben, M. C. Alonso-Garcıa, " A comparative study of the impact of horizontal-to-tilted solar irradiance conversion in modelling small PV array performance", journal of renewable and sustainable energy, 2016, Vol. 8. http://dx.doi.org/10.1063/1.4964363

14. Khalil, S. A. and Shaffie, A. M, " A comparative study of total, direct and diffuse solar irradiance by using different models on horizontal and inclined surfaces for Cairo, Egypt ", Renewable Sustainable Energy Rev, 2013, vol. 27, pp. 853–863. https://doi.org/10.1016/j.rser.2013.06.038

15. Shangyuan Road,” An Economic and Technological Development Zone”, Shaanxi, China.

16. Muna Sabah Kassim, Mustafa Fouad Yousif, Doaa Rokan Hussain, "Numerical study of effect porous media on heat transfer in a horizontal annular tube", Al-Qadisiyah Journal for Engineering Sciences, 2023, vol. 16, pp. 289-297. https://doi.org/10.30772/qjes.2023.143069.1028

17. Sérgio M. O. Tavares, Paulo M. S. T. de Castro, "Equivalent Stress Intensity Factor: The Consequences of the Lack of a Unique Definition", applied Science, 2023, Vol. 13. http://dx.doi.org/10.3390/app13084820

18. Zehnder, A.T, " Fracture Mechanics", Springer Science + Business Media, B.V.: London, UK, 2012. https://doi.org/10.1007/978-94-007-2595-9

19. Perez, N, " Fracture Mechanics", 2nd ed.; Springer International Publishing AG: Cham, Switzerland, 2017. https://doi.org/10.1007/978-3-319-24999-5

20. Krzysztof Rokosz, Tadeusz Hryniewicz, Winfried Malorny, Jan Valiček, Marta Harničárová, " ANSYS analysis of stress and strain after cones plastic deformation", Technical Gazette, 2015, Vol. 22, pp. 503-508. http://dx.doi.org/10.17559/TV-20140211104533

21. Kukiełka, L, Chodor, J, " Numerical analysis of the influence of abrasive grain geometry and cutting angle on states of strain and stress in the surface layer of object", Transactions on Engineering Sciences, 2007, Vol. 55, pp. 183-193. https://doi.org/10.2495/SECM070181

22. Thomas Dawson, Victoria Johnson, Paul Miller, Michael Morabito, Michael Schultz and G.W, " Naval Material Science and Engineering Course Notes ", United States Naval Academy, 2024. https://www.usna.edu/NAOE/academics/en380.php

23. Cooper, P. I, " The Absorption of Solar Radiation in Solar Stills", Solar Energy, 1969, vol. 12. https://doi.org/10.1016/0038-092X(69)90047-4

24. Duffie, John A, and William A Beckman, " Solar Engineering of Thermal Processes", Design Studies, 1982, vol. 3. https://doi.org/10.1016/0038-092x(82)90232-8

25. Gueymard, C.A, " Direct and Indirect Uncertainties in the Prediction of Tilted Irradiance for Solar Engineering Applications", Solar Energy, 2009, vol. 83, pp. 432–444. https://doi.org/10.1016/j.solener.2008.11.004

26. Hottel, H. C, " A Simple Model for Estimating the Transmittance of Direct Solar Radiation Through Clear Atmospheres", Solar Energy, 1976, vol. 18. https://doi.org/10.1016/0038-092X(76)90045-1

27. Iqbal, M, " An Introduction to Solar Radiation", 1983. https://doi.org/10.1016/B978-0-12-373750-2.X5001-0

28. Liu, B.Y.H., and R.C. Jordan, " The Interrelationship and Characteristic Distribution of Direct, Diffuse and Total Solar Radiation", Solar Energy, 1983, vol. 4, pp. 1-19. https://doi.org/10.1016/0038-092X(60)90062-1

29. Maleki, Seyed Abbas Mousavi, H. Hizam, and Chandima Gomes, " Estimation of Hourly, Daily and Monthly Global Solar Radiation on inclined surface ", Energies, 2017, vol. 10. https://doi.org/10.3390/en10010134

30. Spencer, J.W, " Fourier Series Representation of the Position of the Sun", Solar Energy, 1971. http://www.mail-archive.com/sundial@uni-koeln.de/msg01050.html

31. Temps, R.C., and K.L. Coulson, " Solar Radiation Incident upon Slopes of Different Orientations", Solar Energy, 1977, vol. 19, pp. 179-184. https://doi.org/10.1016/0038-092X(77)90056-1

DOI: 10.5281/zenodo.21897816

Appendix

In this appendix, the solar definitions, angles, relations, and irradiance calculation procedure will be explained in detail.

The solar time evaluated from the following relation(Duffie and Beckman 1982):

$$ST = LT + \frac{ET}{60} + \frac{4}{60}[L_s - L_L] \qquad (1)$$

The Equation of Time given as [23]:

$$ET = 229.2(0.000075 + 0.001868 \cos B - 0.032077 \sin B - 0.014615 \cos 2B - 0.04089 \sin 2B) \qquad (2)$$

$$B = (n-1)\left(\frac{360}{365}\right) \qquad (3)$$

The Equation of Hour Angle:

$$\omega = 15^{\circ}(12 - ST) \qquad (4)$$

declination angle can be founded from [24]:

$$\delta = 23.45^{\circ} \sin\left(360\frac{284+n}{365}\right) \qquad (5)$$

The angle between sunbeam radiation on a surface and the normal to that surface. it's obtained from the relation [25]:

$$\cos\theta = \sin\delta \sin\varphi \quad (6)$$

Calculation of the Zenith Angle is below:

$$\cos\theta_Z = \cos\varphi \cos\delta \cos\omega + \sin\varphi \sin\delta \qquad (7)$$

Calculation of the Solar altitude angleis below:

$$\alpha_S = 90^{\circ} - \theta_Z \qquad (8)$$

Displacements east of south are negative and west of south are positive [26].

$$\gamma_S = \sin\omega \left|\cos^{-1}\left(\frac{\cos\theta_Z \sin\varphi - \sin\delta}{\sin\theta_Z \cos\varphi}\right)\right| \qquad (9)$$

A simple equation expressed Normal extraterrestrial irradiance is in the following form [27];

$$G_{On} = G_{SC}(1.000110 + 0.034221 \cos B + 0.001280 \sin B + 0.000719 \cos 2B + 0.000077 \sin 2B) \qquad (10)$$

Where; G_{SC}=1367 W/m^2

Calculation of the horizontal extraterrestrial irradiance is below:

$$G_{Oh} = G_{SC}\left(1 + 0.033 \cos\frac{360\,n}{365}\right) \cos\theta_Z \qquad (11)$$

Calculation of the daily Horizontal extraterrestrial irradiation is below:

$$H_{Oh} = \frac{24 \times 3600 G_{SC}}{\pi}\left(1 + 0.033 \cos\frac{360\,n}{365}\right)\left(\cos\varphi \cos\delta \sin\omega_S + \frac{\pi\omega_S}{180} \sin\varphi \sin\delta\right) \qquad (12)$$

Calculation of the hourly horizontal extraterrestrial irradiation is below:

$$I_{Oh} = \frac{12 \times 3600 G_{SC}}{\pi}\left(1 + 0.033 \cos\frac{360\,n}{365}\right)\left(\cos\varphi \cos\delta\,(\sin\omega_2 - \sin\omega_1) + \frac{\pi(\omega_2 - \omega_1)}{180} \sin\varphi \sin\delta\right) \qquad (13)$$

The atmospheric transmittance is expressed as [28];

$$\tau_b = a_0 + a_1 e^{\frac{k}{\cos\theta_Z}} \qquad (14)$$

Where the coefficients a0, a1, and k are functions for altitude.

r0, r1, and rk are functions for climate type. It's evaluated from Table 4

Table 4. Climate correction factors.

Nomenclature:

ST	solar time	I_c	the total irradiance on horizontal solar panel
LT	the local standard time	I_β	clear sky irradiance on tilted solar panel

DOI: 10.5281/zenodo.21897816

Ls	the standard meridian for a local zone	Ir	ground-reflected radiation
L_L	the longitude of the location	$I_{b\beta}$	direct beam radiation
ET	the equation of time	$I_{d\beta}$	diffused beam radiation
n	the number of the day	*Greek symbols*	
Gsc	solar constant	ω	hour angle
Gon	normal extra-terrestrial irradiance	δ	declination
Goh	horizontal extra-terrestrial irradiance	φ	latitude
Hoh	daily horizontal extra-terrestrial irradiation	β	slope
Ioh	hourly horizontal extra-terrestrial irradiation	γ	surface azimuth angle
τ_b	the atmospheric transmittance	θ	the angle of incidence
I_{cnb}	the clear-sky normal irradiance	θz	zenith angle
I_{cb}	the horizontal beam irradiance	αs	solar altitude angle
I_d	the clear-day diffuse irradiance	γs	solar azimuth angle

DOI: 10.5281/zenodo.21897816